

---

## A simulated investigation on dynamic cutting forces in ultraprecision diamond turning of freeform surfaced optics

S.K. Liu<sup>1</sup>, P. Kanife<sup>1</sup> and K. Cheng<sup>1</sup>

*<sup>1</sup>Department of Mechanical and Aerospace Engineering, Brunel University of London, Uxbridge UB8 3PH, United Kingdom*

*Shangkuan.Liu@brunel.ac.uk, Paul.Kanife@brunel.ac.uk and Kai.cheng@brunel.ac.uk*

---

### Abstract

High precision freeform surfaced components and devices are increasing in demand for various engineering industries, such as consumer electronics, automotive, biomedical engineering, MEMS (micro-electromechanical systems), electro-optics, aerospace and communications. Over the last 10 years or so, it is noticed that ultraprecision manufacturing technology being increasingly well applied to ultraprecision production of mobile phones, security monitor systems, head-up displays (HUD), personalized ophthalmic lenses, and AR/VR/smart glasses in a truly industrial scale. However, it has always been a challenge for precision engineering science to continuously support high precision applications above in a confident manner and to address new challenges resulted from the industrial scale up, such as understanding and monitoring the dynamic cutting forces in the process and working on digital twin of the industrial ultraprecision manufacturing systems. In this paper, a simulated investigation is presented particularly on dynamic cutting forces in ultraprecision diamond turning of freeform surfaced optics and their impacts on various application scenarios. The simulation is developed based on the dynamic cutting forces modelling and analysis against the variations of curvatures in ultraprecision cutting of the freeform surface. The simulation is developed in MATLAB programming environment. The simulations are performed against the industrial application cases including ultrapersonal cutting of an off-axis parabolic mirror (Al alloy). The paper is concluded with the further discussion on the potential and application of this simulation-based approach for ultraprecision machining of freeform surfaced devices and components in an industrial scale.

Cutting force modelling, micro cutting mechanics, ultraprecision cutting, freeform surfaced optics, simulation

---

### 1. Introduction

In recent years, diamond turning has been considered as an efficient industrial approach for machining optical freeform surfaces, although research and development on this method and underlying cutting mechanics are not yet systematic. Optical freeform surface components have attracted more attention due to their high degree of design freedom and compactness. An optical freeform surface is defined as an asymmetrical surface that rotates around an asymmetrical axis or any none-rotationally symmetric surface [1]. Freeform surfaces can also be designed in any shape, and in most cases, these surfaces have submicron profile accuracy and nanoscale surface finishing [2].

The ultraprecision machining systems has become a key enabling technology for machining complex freeform surfaced components or products in an industrial scale, particularly in aerospace, automotive, medical engineering, optics, and microelectronics due to rapidly growing requirement in Micro-Nano manufacturing and smart tooling development. Nevertheless, in terms of optimisation of Fast Tool Servo (FTS) mode machining, Slow Tool Servo (STS) methodology, only a few studies have been transferred to practically fabricate the freeform optical lenses with multi-curvature surfaces. Based on this, it is important that a research on the optimisation and development of an integrated approach to design and precision manufacturing of freeform optical lenses [3].

From the dynamics point of view, the manufacturing of the freeform surface with large depth can be challenging and

difficult in some cases when using diamond turning machine. Therefore, the technology of both FTS and STS diamond turning was developed to overcome and address such challenges in the manufacturing process of freeform optical surface, such as freeform lenses and hybrid surfaces. Nevertheless, these techniques can substantially address the limitation of low bandwidth range in the STS and limited range of stroke in FTS. From another viewpoint, FTS and STS diamond turning process and machining have the highest rate of material removal in comparison with other methods and consequently are widely utilised by researchers and industries.

Within the research and development arena, the cutting force, a critical physical parameter in the machining process, has received substantial attention, however, insufficient effort has been placed on highlighting and exposing the subtle difference of cutting forces and the associated cutting dynamics in ultraprecision diamond turning of freeform surfaces from the perspectives of Fast Tool Servo (FTS) and Slow Tool Servo (STS) machining approaches/application [3]. In the current state of the art in ultraprecision cutting/machining, with the aim of achieving nonmetric level of surface roughness, the Single Point Diamond Tool (SPDT) play a crucial role when compared to other machining approaches/method [3].

Regardless of the impact of the traditional slow tool servo cutting technology in ultra-precision diamond turning, fast tool servo cutting is also employed to achieve high accuracy on complex non-spherical surfaces and microstructures [4]. The cutting tool material of a SPDT machining/cutting process consist of a single crystal diamond with a small diameter cutting

edge and this nanoscale cutting edge of the SPDT tool, makes it possible to facilitate the creation of smooth surfaces with insignificant/slight damage to the top surface [5].

The direct interaction between the cutter and the workpiece holds significant important in single point diamond turning as it relates to the cutting force. The information derived from the tool path data, which is linked to the desired freeform surface, facilitate the emergence of the proposed cutting force model as a promising approach/technique for making sure that the quality control of the designed surface is maintained [3].

The continuous change in surface curvature in freeform surfaces, does present its challenges which is notable in SPDT machining process, leading to dynamic changes and variations in cutting angles during the cutting process. The in-built changes in curvature associated with freeform surfaces directly influence both the cutting angles and the depth of cutting (DoC) of the cutter, have direct effect on the cutting forces throughout the machining operation. Therefore, in-order to accurately predict the cutting force variation across the entire cutting loop, through an analysis of the simulated generated machining process toolpath file, it becomes promising to examine the positional relationships among each cutter location point. This analysis supports in recognising challenging areas on the designed surface. The pros of this proposed approach out weights its cons from an industrial viewpoint, in that its retrospective analysis capability serves as a valuable tool for averting similar challenges in subsequent production cycles, contributing to improved efficiency and product quality. In addition, it provides the platform to retrospectively trace the cutting process, facilitating the identification of factors that may have played a part in the production of faulty parts [3].

There is emphasis and interest recently over the last decade or so on cutting force in single point diamond turning machining technique and span across cutting force control for improved surface results, and the investigation of the relationship between chip loads and cutting force fluctuations and cutting force prediction, analysis of cutter kinematic motion, including cutting force tracking and prediction, etc.

This paper focuses on the variation of the cutting force along the Z-axis as the height position changes in that plane, leading to variations in DoC and angles of kinematics. It also aim at investigating the relationship between the designed freeform surface curvature changes, and the resulting cutting force to enhance the precision and quality of microstructured surfaces.

## 2. Methods

### 2.1. Cutting force and shear force

Atkins' model [6], is the cutting model, on which the cutting force modelling in this study was further developed. Several internal works are identified in cases where surface work plays a substantial role in steady deformation, like: (i) friction along the underside of the chip at the tool interface; (ii) plasticity along the shear plane; and (iii) formation of a new cut surface, as illustrated in Fig. 1. All aforementioned work components are

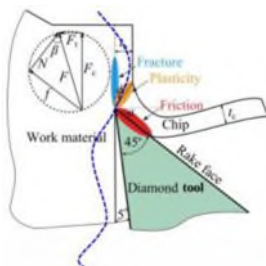


Figure 1. Atkins model cutting application on a freeform surface [6].

externally provided by the  $F_c$  component of the tool force moving along the machined surface's toolpath file. Concurrently, it is important to consider the direction of the cutting force and the practical DoC [3, 6].

### 2.2. Cutting force model in STS process

Based on the toolpath data, to estimate the practical cutting force, it is important to calculate first the practical shear direction using [3, 7]:

$$\phi = \alpha - \theta \quad (1)$$

From equation 1,  $\phi$  represents the friction angle along the rake face, and  $\alpha$  is the tool rake angle.

Concurrently, with the cutter transitioning from the (i-1)-th to the i-th point, the relative distance between these two location points can be calculated using the following function [3, 7]:

$$L = \sqrt{z_1^2 + (x_1 - x_2)^2} \quad (2)$$

where  $f_x$  represents the feed rate along the X-axis of the cutting process, and  $z_1$  and  $z_2$  are the positional data along the Z-axis.

$\theta$ ; which is the included angle between these two points can be written as:

$$\theta = \arctan \left( \frac{z_1 - z_2}{L} \right) \quad (3)$$

The coordinates of the intersection point A ( $X_a, Z_a$ ) between the cutter edge at the previous (i-1)-th point and the current i-th point can be calculated by [3, 7]. See equation (4):

$$\begin{aligned} X_a &= \frac{z_1^2}{2L} - \sqrt{\frac{z_1^2}{4} - (z_2 - z_1)\sin(\theta)} \\ Z_a &= \frac{z_1^2}{2L} (1 + \sin(\theta)) - \sqrt{\frac{z_1^2}{4} - (z_2 - z_1)\cos(\theta)} \end{aligned}$$

The coordinates of the intersection points B ( $X_b, Z_b$ ) and C ( $X_c, Z_c$ ), corresponding to the cutter edge at the preceding (i-1)-th point and the current i-th point, with the uncut surface, can be calculated by [3, 7]:

$$\begin{aligned} X_b &= \sqrt{z_1^2 - (z_1 - h_0)^2} - h_0 \\ Z_b &= h_0 \end{aligned} \quad (4)$$

Where  $h_0$ , is the height of the uncut surface in the toolpath data.

And the relative angle between the i-th point to point A, B, and C respectively can be obtained as [3, 7]:

$$\begin{aligned} \theta_A &= \arcsin \left( \frac{Z_a - Z_i}{L} \right) \\ \theta_B &= \arcsin \left( \frac{Z_b - Z_i}{L} \right) \\ \theta_C &= \arcsin \left( \frac{Z_c - Z_i}{L} \right) \end{aligned} \quad (5)$$

Accordingly, the practical DoC can be calculated by using the equations (7) below [3, 7]:

$$\begin{aligned} DoC &= \frac{1}{2} \left( \frac{z_1 + z_2}{L} \right) \sin(\theta) ; h \leq h_0 \\ DoC &= \frac{1}{2} \left( \frac{z_1 + z_2}{L} \right) \sin(\theta) \end{aligned} \quad (7)$$

Applying Atkins' model, the overall main cutting force can be obtained as follows [3]:

$$F_c = F_{\phi} + F_{\theta} \quad (8)$$

Where:

$V$  = the cutting velocity

$c$  = the horizontal component of the cutting force

$\sigma_y$  = the (rigid-plastic) shear yield stress

$t_0$  = the uncut chip thickness

$\gamma$  = the shear strain along the shear plane; given by  $\gamma = \tan^{-1} \left( \frac{w}{R} \right)$   
 $w$  = the width of the orthogonal cut

$\theta$  = the orientation of the shear plane  
 $R$  = the specific work of surface formation (fracture toughness)

The applied constant parameters used for calculation are listed in Table 1.

**Table 1** Constant parameters using in the calculation

Parameters	Definition	Value
	Spindle rotation (r/s)	3000
	Shear yield (MPa)	55.2
	The coefficient of friction	0.583
$r$	Tool radius (mm)	0.35
	Objective surface diameter (mm)	78
	Tool rake angle (mm)	0

### 2.3. Kinematics of Fast/Slow Tool Servo (F-/STS) and STS process toolpath interpretation and analysis

Throughout the turning process, the material removal zone is defined as the engagement of the cutter areas in any two successive cutting points along the radial direction of the workpiece, and it is equally demarcated into fixed fragments. The kinematics of the F/STS is presented firstly, if the aim is to model the dependent cutting forces for the generation of micro-structured surfaces.

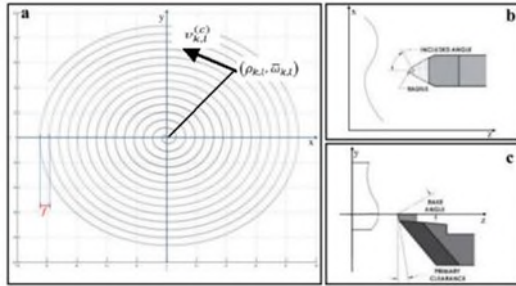


Figure 2. Schematic of diamond turning machining cutting kinematics of (a) the toolpath of the mirror surface in the XOY plane; (b) the surface relationship and the tool-tip at the top view and (c) the cutting process lateral view.

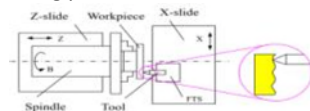


Figure 3. Schematic of FTS mechanism and application on micro-structured NURBS defined surface [8].

As shown in Fig. 2(a&b);  $(x, y, z)$  represent the Cartesian coordinate system fixed on the machine tool, while, the  $(\rho, \theta, z)$  plane is parallel to the planar motion of the slides, and  $z$  corresponds with the spindle axis.

As presented in Fig. 1(a), the turning operation is conducted in a cylindrical coordinate system  $(\rho, \theta, z)$ . By defining and setting  $\rho = R \cos \theta$  and  $z = R \sin \theta$ , the looked-for micro-structured surface can be mathematically described in this cylindrical system as:  $z = f(\rho)$ , where  $f$  implies the mathematical function for the surface [7].

For one revolution of the spindle, the trajectory for F/STS is equally demarcated into  $N$  cutter location points (CLPs). The rounded-edge effect is overlooked for the trajectory calculation, by considering that the edge radius is much smaller than the servo motion.

Assuming that, throughout the cutting process, the cutter tip is aligned with the rotational center, and the CLP is set as the

nose center of the cutter. Furthermore, with the diamond cutter presumed to approaches from the outer space to the center of the workpiece, the radial and angular positions for the  $l$ -th CLP in the  $k$ -th revolution  $(\rho_{k,l})$  can be respectively conveyed by [3, 7]:

$$\rho_{k,l} = R - (l - 1)r \quad (9)$$

$$\theta_{k,l} = 2\pi \left( \frac{l - 1}{N} \right) + \theta_0 \quad (10)$$

Where:

$R$  = the radius of the workpiece  
 $N$  = the angular sampling ratio for one revolution

$f$  denotes the feedrate per revolution along the X-axial direction. At the CLP  $\rho_{k,l}$ , the velocity component induced by the spindle rotation can be expressed by [3, 7]:

$$v_{\theta,k,l} = \frac{2\pi R n}{60} \quad (11)$$

Where  $n$  = the number of revolutions per minute of the spindle.

The conceptualisation of the machine tool trajectory in the slow tool servo mode as shown in Fig.2(a), represent an Archimedes spiral pattern type of motion of the cutter with a cylindrical pattern defined by  $O$  – coordinate system. The XOY plane is aligned parallel to the spindle surface within this coordinate system. Along the X-axis direction (either from the centre to the edge or vice versa), the cutter movement follows a linear motion with uniform speed on this XOY plane. In the C-axis, this described motion is coordinated with the rotational movement of the spindle with this axis [3].

The cutter location point (the point of engagement between the cutter and the workpiece) can also be located as shown in Fig. 2(a). Furthermore, as depicted in Fig.2(a), the trajectory of the machine tool in STS mode can be conceptualized as the Archimedes spiral pattern motion of the cutter within the  $(\rho, \theta, z)$  cylindrical coordinate system. In this system, the XOY plane is aligned parallel to the spindle surface. On this plane, the cutter's movement follows a linear motion with uniform speed along the X-axis direction (either from the center to the edge or vice versa). This motion is coordinated with the rotational movement of the spindle in the C-axis. An Archimedean spiral pattern of motion is created as a result of this movement with a predetermined distance between each point and a specified feed rate. The tool radius plays an important role in relation to the feed rate which, in turn, has a significant impact on the resulting quality and processing time of the machine. These parameters considerably effect the number of points in each circle and the number of circles the cutter needs to traverse [3].

In addition, from Fig.2(b&c), both planes jointly depict the motion of the cutter along the Z-axis direction. The XOZ plane illustrates the correlation between the tool radius and the movement along the X-direction while the YOZ plane runs parallel to the plane defined by the cutting edge of the tool. Bearing in mind the interplay between tool geometry and the chosen toolpath strategy, optimizing and understanding these trajectories are crucial for achieving precise and efficient machining [3].

## 3. Results and discussion

### 3.1 Experimental setup

The workpiece to be machined is an off-axis parabolic mirror (Al alloy) and the cutting tool is diamond. The virtual cutting simulation and the generation of the tool path, cutter location and the G-code is achieved using NanoCam industry standard software which has the capability to carryout ultraprecision diamond turning simulation that mimic the F-/STS cutting kinematics. Matlab script was written to analyse the generated tool path/cutter location point and the cutting force is calculated using the Atkins model cutting force equation (see equation 8)

with inputted parameters while considering the variation in shear angle.

The mirror surface machining procedure that employs a carrier disk is highlighted in Fig. 4(a), which demonstrates the cutting motion in the process. The diameter of the disk is 290 mm, as shown in Fig. 4(b), and the carrier disk has the capacity to hold six mirrors which allows the machine to work on them simultaneously. The mirrors are arranged and distributed symmetrical from left to right, with two mirrors allocated on the top and bottom (position at  $35.65^\circ$  apart) and one each on the left and right and (positioned at  $72^\circ$  apart). During machining, the cutter continuously transitioning between kinematic motion and movement toward the next surface working/cutting concurrently on six mirrors within the container [3].

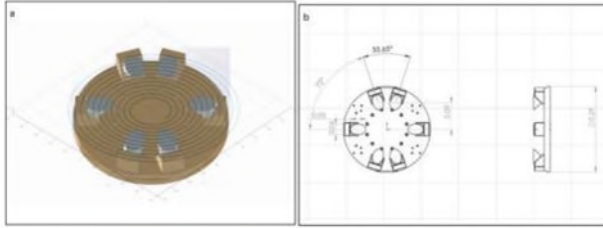


Figure 4. (a) Virtual simulation cutting motion and mirror surface machining procedure with a carrier disk and (b) Spread of the workpieces on the carrier disc and associated parameters

### 3.2 Modelling results and discussion

It is observed that the cutting force within the selected estimated section, corresponds to the movement of the tool along the x-axis, ranging from 18.76 cm to 18.90 cm respectively (using 206,460 of the cutter location points). Nevertheless, Fig. 4, portrays the estimated primary cutting force and demonstrates an estimable accordance, reflecting the variations in cutter kinematics perfectly especially when it moves between each surface without any cutting progress [3].

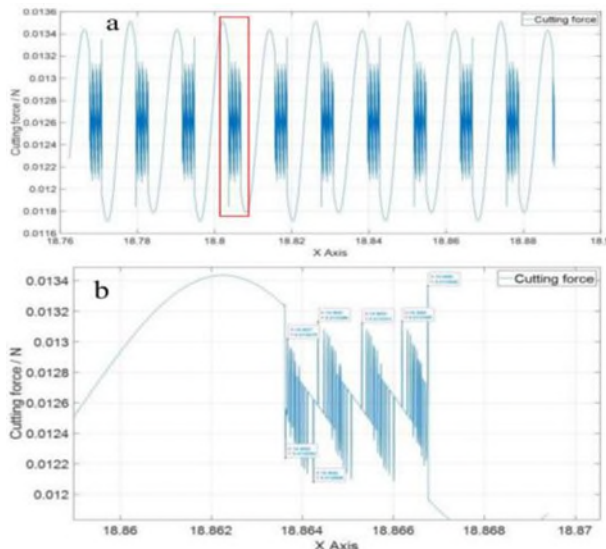


Figure 5. The estimated cutting force characteristics. (a) Depiction of the cutting force from 18.76 cm to 18.9 cm and (b) The cutting force plot with focus only on the red frame part (from 18.86 cm to 18.87 cm).

As indicated in Fig. 5(a), a specific loop was selected within the cutter location on the X-axis between 18.86 cm and 18.87 cm range. This focused selected range, provide a detailed insight into the characteristics of the cutting force as it changes as the cutting process progresses, with additional focus on the material being removed on the surface. Furthermore, it is clearly observed based on the nature of the cutting motion, that the estimated minimum cutting force occurs at 18.8642 cm along

the X-axis which represent the position of the cutter and at this point, the cutting force is recorded as 0.0120778 N [3].

The rising fashion of the cutting force becomes negative, eventually showing a decline, as the practical shear angle decreases as shown in Fig. 6. It is observed, that the change in shear angle becomes more frequent but remain subtle, therefore making it difficult to immediately understand as the cutter moves into the material removal area. This behaviour also applies to the cutting force at those points of reference. With this in mind, the developed model cleverly captures the cutters location based on the cutter tool path data, not forgetting the process parameters associated with diamond turning material removal process during the machining process based on the observed findings [3].

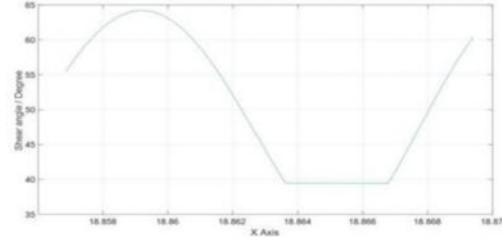


Figure 6. Change in angle of the practical shear

### angle. 4. Conclusions

This paper presents innovative cutting force modelling, takes account of the influence of the surface curvatures and thus cutting angles variations encountered in ultraprecision diamond turning of freeform surfaces. Simulations and experimental work are thoroughly investigated and analysed. MATLAB/ Simulink programming is employed for developing the simulations based on improved Atkins model while dedicated in cutting forces modelling for diamond turning freeform surfaces.

Currently, there is an ongoing effort on further improving the modelling by combining with digital twin and in-process machining data, which will be reported separately in the near future.

### References

- [1] Garrard, K., Thomas, B., Jeff, H., Thomas, D., and Alex, S., (2005) "Design tools for freeform optics," in *Proceedings of the Current Developments in Lens Design and Optical Engineering VI*, vol. 5874, pp. 1–11, SPIE, San Diego, CA, USA, August 2005.
- [2] Jiang, X., Paul, S., and David, J. W., (2007) "Freeform surface characterisation, a fresh strategy," *CIRP Annals*, vol. 56, no. 1, pp. 553–556, 2007.
- [3] Shangkuan, L., Kai, C., and Joe, A., (2024) Modelling and analysis of cutting forces in ultraprecision diamond turning of freeform surfaces and their assessment. euspen's 24<sup>th</sup> International Conference & Exhibition, Dublin, IE.
- [4] Gong, Z., Huo, D., Niu, Z., Chen, W., & Cheng, K. (2022). A novel longstroke fast tool servo system with counterbalance and its application to the ultra-precision machining of microstructured surfaces. *Mechanical Systems and Signal Processing*, 173, 109063.
- [5] Yip, W. S., Yan, H. E., Zhang, B., and To, S. (2024). The state-of-art review of ultraprecision machining using text mining: Identification of main themes and recommendations for the future direction. *Wiley Interdisciplinary Reviews: Data Mining and Knowledge Discovery*, 14(1), e1517.
- [6] Atkins, A. G. (2003). Modelling metal cutting using modern ductile fracture mechanics: quantitative explanations for some longstanding problems. *International journal of mechanical sciences*, 45(2), 373–396.
- [7] Zhu, Z., To, S., Zhu, W. L., Huang, P., & Zhou, X. (2019). Cutting forces in fast/slow tool servo diamond turning of micro-structured surfaces. *International Journal of Machine Tools and Manufacture*, 136, 62–75.
- [8] Sawangsri, W. and Cheng, K. (2016). An innovative approach to cutting force modelling in diamond turning and its correlation analysis with tool wear, *Proceedings of the IMechE, Part B: Journal of Engineering Manufacture*, 230(3), 405–415.